Supplementary material for: "*Estimating the elastic modulus of landfast ice from wave observations*", by Voermans et al.

SUPPLEMENTARY MATERIAL

Part 1. Numerical simulations of vibrating fixed-ends beam

The 3D computation domain of round shape (S) used in numerical simulations is shown in Fig. 1. The radius and the thickness of the computation domain were respectively 10 m and 0.3 m. The thickness of the computation domain equals the ice thickness h_i. The fixed-ends beam is located between two parallel vertical cuts with round ends. The widths of the beam and the cuts were respectively $w = 0.27$ m, and $d = 0.1$ m (Fig. A1a). Numerical simulations were performed using Solid Mechanics and Structural Mechanics modules of finite element software Comsol Multiphysics 5.4. Figure S2a shows physically controlled tetrahedral mesh with extra fine resolution used in the numerical simulations. Figure S2b shows the mesh in the vicinity of the ends of two parallel cuts and near the beam root.

The ice rheology is described by isotropic elastic material. Numerical simulations were performed to find eigen frequencies and to demonstrate that time-dependent problem with specific boundary condition leads to the generation of the first eigen mode of flexural oscillations of the beam. Elastic rheology of ice is characterized by the elastic modulus E, the Poisson's ratio ν, and the ice density ρ_i. In the simulations the ice density was set to $\rho_i = 920$ kg/m^3. It is known that eigen frequencies of bending oscillations of elastic beams are determined by the elastic modulus and the beam geometry (Landau and Lifshitz, 1964). Therefore, in the simulations the Poisson's ratio was set to the constant value $\nu = 0.35$.

At the outer round face of domain S low-reflecting boundary condition was set. Free surface boundary condition was set at the top surface of the computational domain and at the lateral surfaces of the vertical cuts. In time dependent simulations localized external loads were applied to the beam and to the ice to initiate vertical motion. The loads were applied over gray rectangles S_f with sizes 0.1 m x 0.27 m (Fig. A1a). The loads increased linearly from 0 to 1000 kg during 0.001 s and then dropped to 0. The loads applied to the beam and to the edge of ice plate were opposite directed. At the bottom surface of computational domain, the condition of spring foundation with elastic constant of 10000 N/m^3 was used to imitate the buoyancy force acting on the ice bottom. In addition, the added mass condition with the added mass of 320.7 kg/m^2 was used (Fig. A1b).

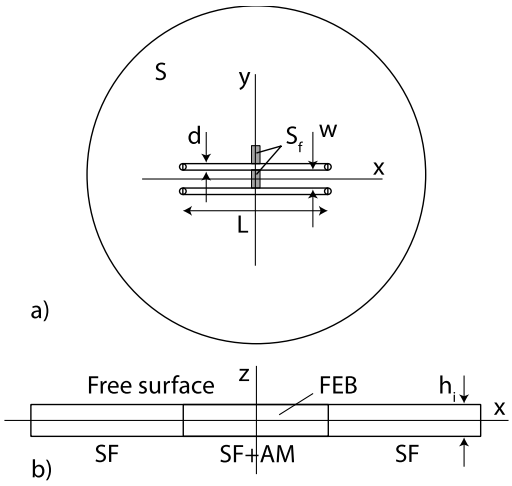

Figure S1. Projection of computational domain on horizontal (a) and vertical planes (b).

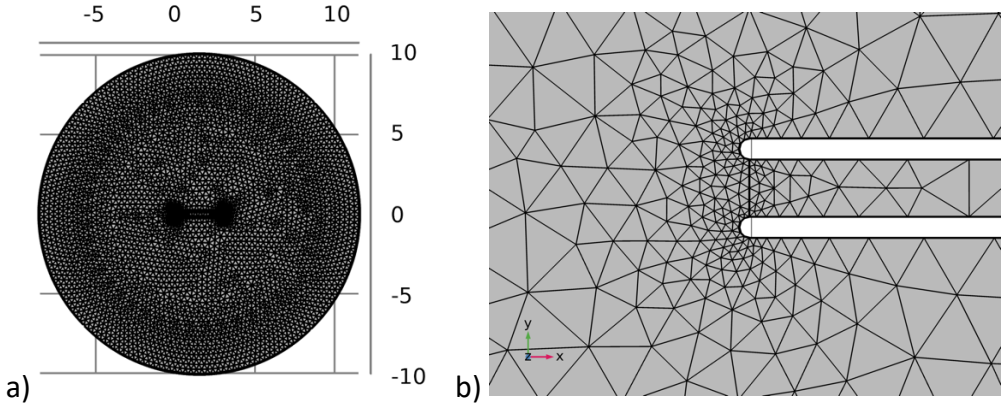

Figure S2. Physic-controlled mesh with extra fine resolution used in numerical simulations.

Figure S3 shows results of the eigenfrequency study. Among many eigen modes of the computational domain we selected the mode with maximal deformation of the fixed-ends beam in the center and minimal deformation of surrounded ice. Figure S3a shows the shape of such mode having eigen frequency 17.2+0.19i Hz along the x-axis. The eigen frequency is complex because low-reflecting boundary condition allows energy sink through the periphery face of the computational domain. The eigen mode was calculated with the elastic modulus $E = 1.1$ GPa. Figure S3b shows the dependence of the elastic modulus E from the real part of the eigen frequency f.

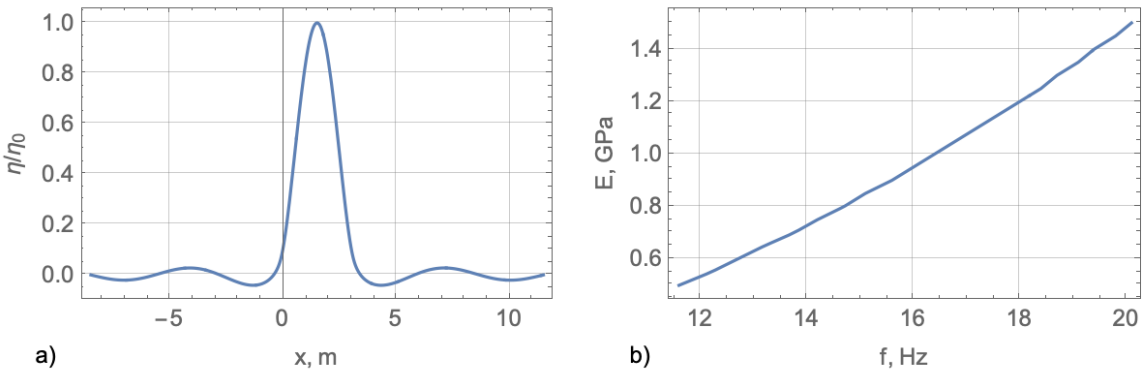

Figure S3. Shape of the first eigen mode of flexural oscillations of the fixed-ends beam along the x-axis (a). Dependence of elastic modulus from of the first eigen mode frequency (b).

Figure S4 shows results of numerical simulations of the initial value problem. Blue line in Figure S4a shows normalized non-dimensional displacement of the beam center from time. Yellow line in Figure S4a shows normalized non-dimensional displacement of the closest point at the ice edge cross the cut. Figure S4b shows the shape of the beam axis and surrounded ice along the x-axis in two times different on the half period of the oscillation. One can see that the amplitude of vertical oscillations of the beam center is much greater the amplitudes of vertical oscillations of surrounded ice. Figure S5 shows spectrum of the graph in Fig. A4a. Spectral maximum is reached at $f \approx 18$ Hz what is higher than 17.2 Hz obtained for the eigen frequency. The difference can be explained by error accumulation during numerical simulations of oscillating solution of time dependent problem, and finite dimensions of the computational domain influencing many additional eigen frequencies in addition to the eigen frequency of the fixed-ends beam in unlimited ice plate.

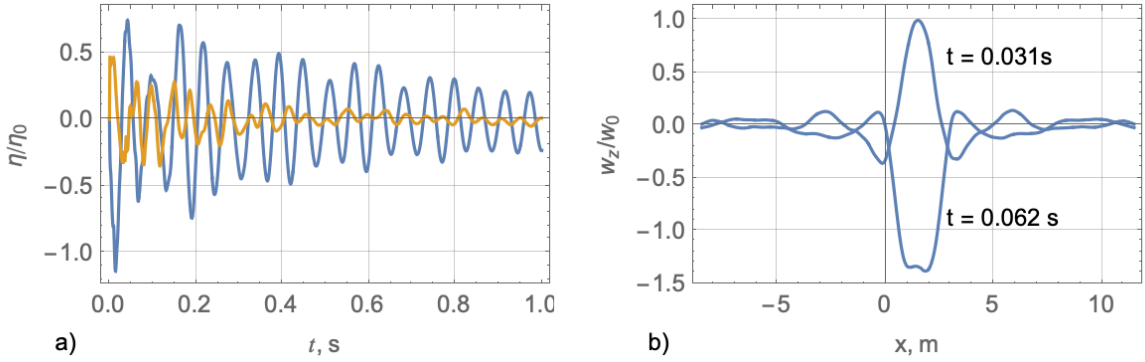

Figure S4. Normalized vertical displacement of the beam center (blue line) and closest point at the ice edge (yellow line) versus time calculated with $E = 1.1$ GPa (a). Spectrum of the normalized vertical displacement (b).

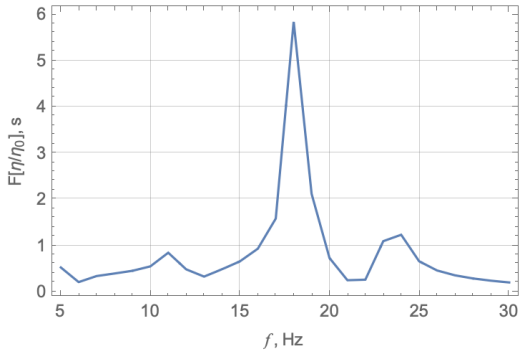

Figure S5. Spectrum of the normalized vertical displacement.

Part 2. Calculation of added mass

The added mass effect should be considered when the flexural oscillations of floating beams are calculated. The added mass per unit area of the beam surface is expressed by the integral (Marchenko et. al, 2020)

$$m_{ad} = \frac{2\rho_w w}{\pi^2} \int_0^\infty \int_0^\infty \frac{(\sin u)^2 (\sin v)^2}{u^2 v^2 \sqrt{(uw/L)^2 + v^2}} du\, dv. \quad \text{(A1)}$$

Numerical calculations using NIntegration in Wolfram Mathematica shows that $m_{ad} = 320.7$ kg/m^2 when $\rho_w = 1030$ kg/m^3, $L = 3$ m, and $w = 27$ cm. This value of the added mass was used in numerical simulations.

The frequency dependence of added mass appears when the energy of oscillations of a floating/submerged body is radiated into surface and acoustic waves. Surface wave effect is important when there is free surface, and the frequency is low. For the high frequencies the dynamic boundary condition at the free surface turn to equality of the velocity potential zero (Newman, 2017, Fig. 6.22), and the added mass in the vertical direction is similar the added mass of a body in unlimited fluid. Figure 6.23 in Newman (2017) estimates frequency limit for the sphere with diameter d. The added mass is closed to the standard value $\pi d^3/12$ when $\omega^2 d/g = 6$. Assuming $d = 1$ m we find that $\omega/2\pi = 1.3$ Hz. It is much lower the frequencies measured in the tests with fixed-ends beams. Radiation of acoustic waves is important for bodies with very small mass submerged in a liquid with large density (Golyamina and Issakovitch M.A., 1981).

References

Golyamina, I.P., Issakovitch, M.A., 1981. *Frequency characteristics of mechanical harmonical oscillator immersed in acoustic medium*. Acoustic Journal, Vol. XXVII, N 5, p. 730-735

Landau, L.D., Lifshitz, E.M., 1975. *Theory of elasticity*. Pergamon Press, Oxford, 165 pp.

Newman,J.N., 2017. *Marine Hydrodynamics*, The MIT Press Cambridge, 426 pp.

Marchenko, A., Karulin, E., Chistyakov, P., Karulina, M., Sakharov, A., 2023. *Meso-scale stress relaxation test on floating sea ice*. POAC-23.

Marchenko, A., Grue, J., Karulin, E., Frederking, R., Lishman, B., Chistyakov, P., Karulina, M., Sodhi, D., Renshaw, C., Sakharov, A., Markov, V., Morozov, E. G., Shortt, M., Brown, J., Sliusarenko, A., Frey, D., 2020. *Elastic moduli of sea ice and lake ice calculated from in-situ and laboratory experiments*. Proceedings of the IAHR International Symposium on ice 2020.

Voermans, J., Liu, Q., Marchenko, A., Rabault, J., Filchuk, K., Ryzhov, I., Heil, P., Waseda, T., Nose, T., Kodaira, T., Li, J., Babanin, A.V., 2021. *Wave dispersion and dissipation in landfast ice: comparison of observations against models*. The Cryosphere, 15, 5557–5575.